Received: 27 September 2021 | Revised: 12 June 2022 | Accepted: 15 June 2022

DOI: 10.1111/ejss.13269

ORIGINAL ARTICLE

European Journal of Soil Science WILEY

Millimetre scale aeration of the rhizosphere and drilosphere

Daniel Uteau[1] | **Rainer Horn**[2] | **Stephan Peth**[3]

[1]Department of Soil Science, Faculty of Organic Agricultural Sciences, University of Kassel, Witzenhausen, Germany

[2]Institute of Plant Nutrition and Soil Science, University of Kiel, Kiel, Germany

[3]Institute of Soil Science, Faculty of Natural Sciences, Leibniz University Hannover, Hannover, Germany

Correspondence
Daniel Uteau, Department of Soil Science, Faculty of Organic Agricultural Sciences, University of Kassel, Nordbahnhofstr. 1a, 37213 Witzenhausen, Germany.
Email: uteau@uni-kassel.de

Funding information
Deutsche Forschungsgemeinschaft, Grant/Award Number: DFG PAK888

Abstract

Soil aeration is a critical factor for oxygen-limited subsoil processes, as transport by diffusion and advection is restricted by the long distance to the free atmosphere. Oxygen transport into the soil matrix is highly dependent on its connectivity to larger pore channels like earthworm and root colonised biopores. Here we hypothesize that the soil matrix around biopores represents different connectivity depending on biopore genesis and actual coloniser. We analysed the soil pore system of undisturbed soil core samples around biopores generated or colonised by roots and earthworms and compared them with the pore system of soil, not in the immediacy of a biopore. Oxygen partial pressure profiles and gas relative diffusion was measured in the rhizosphere and drilosphere from the biopore wall into the bulk soil with microelectrodes. The measurements were linked with structural features such as porosity and connectivity obtained from X-ray tomography and image analysis. Aeration was enhanced in the soil matrix surrounding biopores in comparison to the bulk soil, shown by higher oxygen concentrations and higher relative diffusion coefficients. Biopores colonised by roots presented more connected lateral pores than earthworm colonised ones, which resulted in enhanced aeration of the rhizosphere compared to the drilosphere. This has influenced biotic processes (microbial turnover/mineralization or root respiration) at biopore interfaces and highlights the importance of microstructural features for soil processes and their dependency on the biopore's coloniser.

KEYWORDS

biopore, earthworm hole, pore connectivity, root path, X-ray CT

1 | INTRODUCTION

Soil structure is the key factor for all transport mechanisms including aeration. Structure formation may occur due to abiotic and biotic processes. On the abiotic side, we have the rearrangement of particles and voids, resulting in the formation of soil units called aggregates (Horn et al., 1994; Larney, 2007) and secondary interaggregate pores. Structure formation is furthermore enhanced by the biological activity of meso/macrofauna and flora,

especially by the formation of biopores (pores created by the action of the biota), which are suggested to be more relevant for larger scales (Oades, 1993). Macrofauna, especially earthworms, are large enough to move soil particles and directly create cylindrical, large and continuous pores. Earthworms create and modify the biopore surroundings by laterally compacting it and covering biopore walls with secretions. The soil around this kind of biopore is called the drilosphere (Andriuzzi et al., 2013). Also, plant roots create biopores by pushing soil particles aside and altering the surrounding soil matrix with secondary lateral root channels. The soil affected by this action is called the rhizosphere (Hinsinger et al., 2009). Rooting generates large, continuous and highly connective pore networks enhancing water and air flow (Carminati et al., 2009). After decomposition, old root channels become a passage for new roots and earthworms (Pagenkemper et al., 2015; White & Kirkegaard, 2010) resulting in a continuous reorganisation of associated pore spaces. Roots can also indirectly form pores by enhancing crack formation through water extraction and intense drying/wetting cycles (Beck-Broichsitter et al., 2020; Rasse et al., 2000; Uteau et al., 2013). Gradients in matric potentials were reported at the root surface with pF values near the wilting point while the bulk soil still showed matric potentials around pF = 3 (Carminati et al., 2011). Thus, water extraction from the surrounding soil results in failure generation parallel to the root axis (Helliwell et al., 2019). With repeated wetting/drying cycles also perpendicular and shear failure occur. These direct and indirect forms of pore generation by roots are called root-induced-macropores (RIMs) (Rasse & Smucker, 1998) and are ecologically relevant due to their high connectivity. The practical use of this feature is frequently associated with cropping systems for sustainable agricultural practices (Yunusa & Newton, 2003). Pre-crop sequences with taproot plants such as alfalfa (*Medicago sativa*) or chicory (*Cichorium intybus*) can have beneficial effects on subsequent crops as 20% increased yield or even more are documented (Kirkegaard et al., 2008). According to (Materechera et al., 1992), thicker taproots can better penetrate into highly resistant soil layers and thus create RIMs in the subsoil. After two years, alfalfa roots may grow deeper than 1.40 m (Pietola & Smucker, 1995) with averages of 2–4 m (Heichel, 1980) and maximum depths of 9 m (Kutschera & Lichtenegger, 1992). Other taproot plants like chicory have been reported to grow down to 1.60 m (Hackett, 1982) and even 2 m (Han et al., 2015). Biopores generated by earthworms can reach depths of 2 m (Butt & Grigoropoulou, 2010) and are contrastingly mostly characterised by the absence of lateral channels and smooth walls due to earthworm excretions and their movement activities (Andriuzzi et al., 2013). Thus, the surrounding microenvironment of biopores may show distinct pore systems as a function of their genesis.

Mass flow and diffusion of oxygen highly depend on soil structural parameters related to air-filled porosity, pore geometries, soil strength and accessibility of pore surfaces on the macro- and microscale. Frequently, aeration parameters are related to the fraction of air-filled porosity as it is the most obvious compartment for gas transport. However, the geometry of the air-filled porosity is also known to affect gas transport (Eden et al., 2012). For example, pore size distribution is especially important for mass flow as the flow rate is related to the fourth power of the pore radius (Horn, 1994). Also, the orientation of pores has an influence on airflow, particularly in cases of soil compaction, leading to anisotropic transport properties (Dörner & Horn, 2009). Other well-documented structure characteristics for air transport are connectivity and tortuosity of the pore system (Horn & Peth, 2009; Peth et al., 2008).

Most studies on the relationship between pore geometries and flow properties in soil concentrated on the bulk soil. Yet an open question still remains on how soil structural attributes influence flow processes at the interface between biopores and bulk soil, that is, within the rhizosphere or drilosphere, respectively. Although we have a fair knowledge about the main flow path across the soil profile, we lack information about small-scaled flow paths and the accessibility of the pore wall and its adjacent soil volume, where we find a high biological activity which depends on oxygen supply. The interface of biopores has a special microstructure that is influenced by worms and roots which both enter a bulk soil by penetrating it and pushing aside soil particles, thus increasing the bulk density of the surrounding soil radially (Bruand et al., 1996; Dorioz et al., 1993; Young, 1998). For example, Bruand et al. (1996) found an increase in bulk density of 0.3 g cm^{-3} in the soil next to the root. Those biopores are characterised by an immediate alteration of the surrounding soil by a reorientation of aggregates and particles. These are now aligned parallel to the interface and cause anisotropy in the microstructure. Nevertheless, according to recent observations with non-invasive techniques such as X-ray computed tomography (X-ray CT), differences in the biopore-to-soil-matrix interface were found as a function of pore genesis (Haas & Horn, 2018). The soil matrix surrounding a root path presented a highly complex pore network (visually assessed), while on the contrary, earthworm holes had a smoother surface because of the worm's excretions that sealed many surrounding lateral pores. Also, the continuous friction due to the worm's repeated passing prevented the generation of lateral pores over time. Thus, we hypothesize that biopores generated or colonised by root activity have a

denser and more connective pore network around them than biopores generated or colonised by earthworms and as the bulk soil. The objective of this study was to investigate microscale pore networks in the rhizosphere and drilosphere combining microsensing techniques and X-ray CT. In this study, we refer to biopores as those of first-order which commonly have diameters of 5–10 mm. This was done that way, because of the investigated scale (mm) and the X-ray CT resolution.

2 | METHODS

2.1 | Site description, sampling and sample preparation

The study site was located at the central field trial CeFiT of the University of Bonn (site Klein-Altendorf, Germany. 6°59′29″N, 50°37′21″E) which was established in the frame of a research unit studying the effect of tap-root and shallow-root precrops on subsoil structure formation and its influence on nutrient acquisition. The soil type was haplic Luvisol (IUSS Working Group WRB, 2015), which is characterised by a silty clay loam texture with clay accumulation in the subsoil (50–95 cm depth). Selected plots were cultivated since 2007 with alfalfa (*Medicago sativa*) or chicory (*Cichorium intybus*) up to the sampling date in 2010 (two growing periods). In each treatment, six undisturbed soil cores (10 cm Ø, 10 cm height) were taken vertically at 45–60 cm depth with an Eijkelkamp® steel auger. Two of the six cores of each treatment were selected, water-saturated from below in the laboratory and placed on porous ceramic plates at a matric potential of −150 hPa for drainage.

2.2 | X-ray computed tomography (X-ray CT)

The samples were analysed by X-ray CT with a *phoenix nanotom*® (Phoenix-X-ray, GE Sensing & Inspection Technologies GmbH, Wunstorf, Germany) at the Institute of Plant Nutrition and Soil Science, CAU Kiel, Germany. The scans of the drained samples were done at an energy level of 105 keV and a current of 225 µA with a 0.1 mm copper filter between the X-ray source and the sample. A total of 1441 projections with 1 s exposure each were taken. The drainage of −150 hPa matric potential guaranteed a reduced X-ray scattering which often occurs at high water content. Because the samples did not shrink during drainage, a rigid soil structure could be assumed. Image 3D reconstruction was done with datos|x (GE-Sensing and Technologies GmbH, Wunstorf, Germany), using a modified Feldkamp back-projection algorithm. The achieved voxel edge size was 64.65 µm.

2.3 | Microsite selection and micro oxygen diffusion measurements

After X-ray CT scanning, the samples were rewetted from below and drained to −60 hPa on ceramic plates. This allowed the calculation of the air-filled porosity from the difference between the total porosity and the water content at −60 hPa. At a millimetre scale, three conditions were selected: (1) biopores generated or colonised by earthworms and their adjacent drilosphere (2) biopores generated or colonised by roots and their adjacent rhizosphere, and (3) structured bulk soil (not in the immediacy of a biopore). The type of biopore was assessed visually. To be sure to classify a pore as "generated or colonised by earthworms", we only selected biopores containing fresh earthworm casts on the pore wall. To be sure to classify as "colonised by roots", we only selected biopores still containing remains of the fresh root. An example of both types of pores is given in Figure S1A,B. This allowed us to be sure of investigating recently (fresh) colonised biopores, as we considered the last coloniser to be mostly responsible for the connectivity of the lateral pores. We selected only first-order biopores with diameters ranging between 5.4 and 10.9 mm. As the number of soil cores was limited, and we only selected pores which could be safely classified, there was a very limited number of pores to analyse. Thus, for each treatment, only 3 biopores of each kind were selected.

Once the pores were classified, on the upper end of the biopore (i.e., on the top of the core) one side of the biopore was partially removed to expose the other side to measure perpendicular micro profiles of oxygen partial pressure (pO_2) in the transition region between the biopore wall and the bulk soil. For this purpose, Clark-type needle microelectrodes with a tip size of 100 µm (Unisense A/S, Aarhus, Denmark) were inserted slowly into the soil by a computer-driven micro-manipulator with a precision of 1 µm (Figure S1D). The micromanipulator was stopped at distance intervals of 100 µm for 5 s to let the sensor take a pO_2 reading before continuing with the next location. For each microsite, a total of six profiles (2 in each biopore) up to 20 mm depth were measured.

Close to the pO_2 microprofiles, soil oxygen diffusion coefficients (D_S) were measured as a function of the distance to the free atmosphere. Fickian diffusion coefficients in soils are normally measured in chamber setups where gases are allowed to diffuse across a sample. In this case, this was not possible as only one end of the

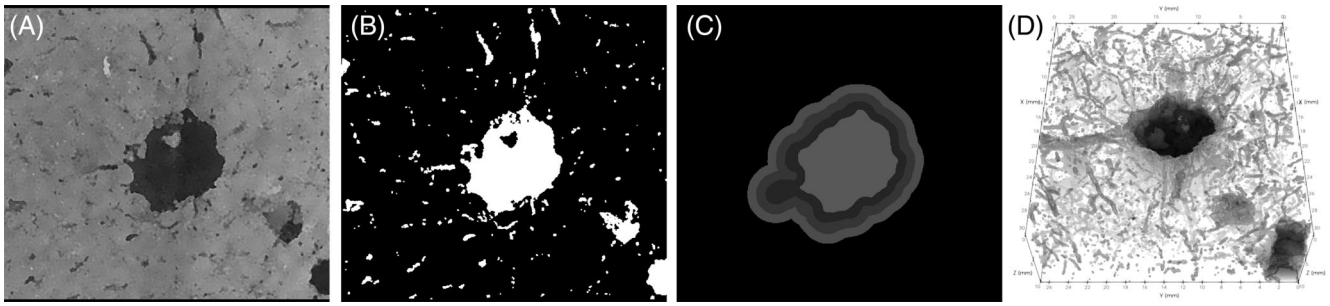

FIGURE 1 Image processing steps. (a) Selection of a region of interest and noise reduction. (b) Segmented binary image (pores in white, soil matrix in black). (c) Isolation of the central pore and generation of radial masks. (d) 3D rendering of the biopore (here a root colonised biopore) and surrounding CT-porosity

sample was exposed (the biopore's surface), thus the approach of Rappoldt (1995) adapted to pore surfaces as suggested by Haas and Horn (2018) was used. As this measurement is far more complex and time-consuming than the pO_2 profiles, one millimetre penetration steps were used instead. Two oxygen sensors were used for this measurement. One sensor tip was placed on the "free atmosphere" very close to the pore surface while the second was inserted one millimetre with the same micromanipulator as described above. The samples and sensors were separated from the room atmosphere by a self-made Plexiglas chamber with a three-way valve gas inlet (Figure S1C) to flush synthetic air (20.5% O_2 and 79.5% N_2) or technical nitrogen (99.8% N_2). The gas flux through the chamber was changed slowly from air to N_2 and back until sinusoidal-like curves of pO_2 with phases of 30 s were registered by both sensors. This was achieved after 2–3 cycles. Oxygen diffusivity was calculated from the distance-normalised phase shift between the surface and the inserted sensor analogous to the one-dimensional heat transport equation (Rappoldt, 1995). Thereafter, the inserted sensor was pushed another millimetre into the soil matrix and the measurement was done again. This was repeated until the inserted sensor did not respond to the pO_2 concentration changes in the chamber, which was usually around 4–6 mm from the pore surface. The oxygen diffusivity was multiplied by the sample's porosity to obtain D_S at each insertion point. D_S was normalised by the oxygen diffusion in pure air ($D_O = 2.01 \times 10^{-5}$ m^2 s^{-1}) resulting in the relative diffusion coefficient (D_S/D_O). For each treatment (alfalfa and chicory) and site, three (one per biopore) micro-diffusion measurements were done.

2.4 | 3D-Image analysis

Image analysis was done in ToolIP®2018 (Tool for Image Processing, Fraunhofer Institute for Industrial Mathematics, Kaiserslautern, Germany) where multiple image processing algorithms can be connected forming flowchart networks. Image noise was reduced by a median filter with a window size of 3^3 voxels (Figure 1a). Afterwards, a region of interest (ROI) was selected containing 1–2 cm of the same biopores described in section 2.3 and their adjacent 6–10 mm soil matrix. The images were segmented using Otsu's threshold algorithm (Otsu, 1979) resulting in an image containing the biopore and X-Ray CT resolved pores (hereafter referred to as CT-porosity) in the rhizosphere and drilosphere, from which the biopore's surrounding CT-porosity could be calculated (Figure 1b). A volume filter applied after labelling (also known as connected components labelling in other software packages) was applied to remove isolated pores, thus resulting in an image containing only the biopore and connected lateral pores from which the biopore connected CT-porosity could be calculated. The biopore in each ROI was isolated from the rest of the matrix and lateral pores by a spherical opening morphological filter of size 20 voxels followed by filling isolated gaps in the biopore with the local-minima plugin. The biopore was successively dilated in 1 mm steps with a dilation morphological filter, analogous to the steps used for the micro diffusivity measurements. For each dilation, step a mask was created to subtract the CT-porosity and the connected-CT-porosity from the original images (Figure 1c). This information was used as a proxy for the potential aeration of each microsite. Image rendering (Figure 1d) was performed in Paraview 5.9 (Kitware Inc., New York, USA).

3 | RESULTS

At the microscale, the evaluation of the three chosen microsites (bulk soil matrix, earthworm or root generated/colonised biopore) showed differences in CT-porosity and pore geometries which play a fundamental role in the aeration at the millimetre scale.

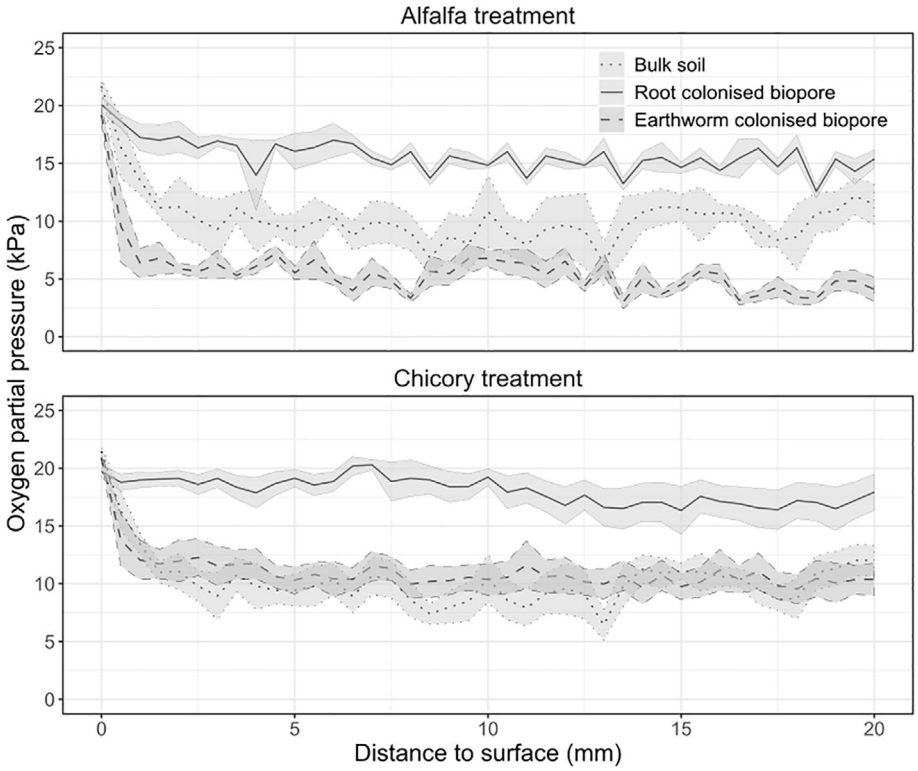

FIGURE 2 Oxygen partial pressure (pO_2) profiles as a function of the distance to the biopore surface (free atmosphere) in an eluviated horizon of a haplic Luvisol for Alfalfa (top) and Chicory (bottom). Samples were drained to a matric potential of −60 hPa. Lines represent averages and shaded areas represent standard error of the mean ($n = 6$).

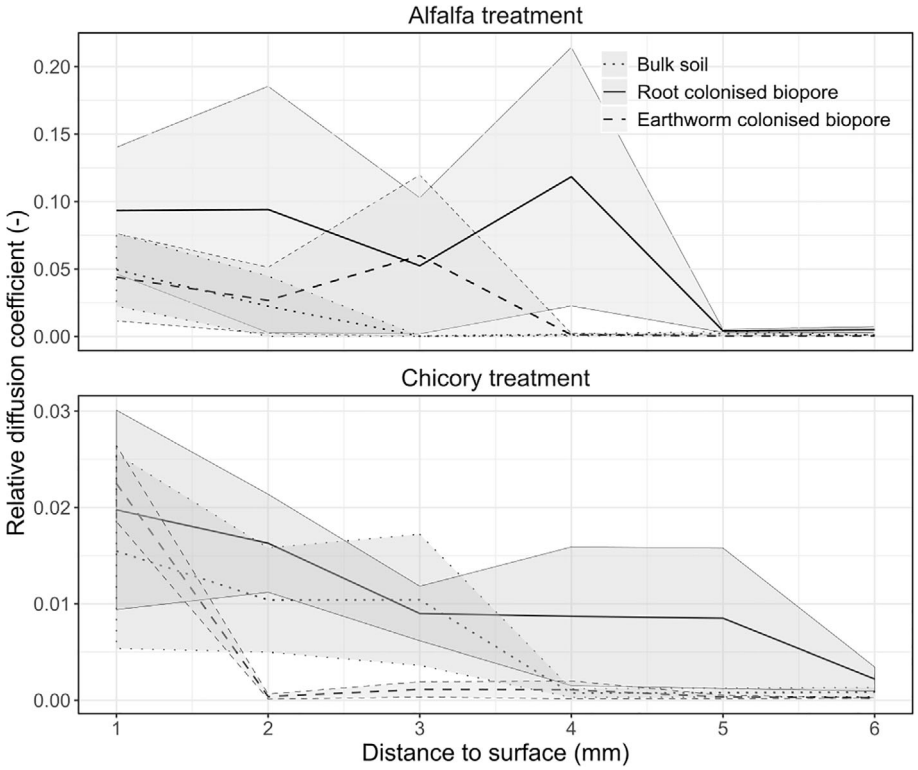

FIGURE 3 Relative diffusion coefficient (D_S/D_O) profiles as a function of the distance to the surface (free atmosphere) in an eluviated horizon of a haplic Luvisol. Note the different Y-axis scales. Samples drained to a matric potential of −60 hPa. Lines represent averages and shaded areas represent standard error of the mean ($n = 3$).

Profiles of pO_2 on the structured soil samples showed that oxygen concentration in the bulk soil was 5–10 kPa higher for root colonised biopores compared with earthworm colonised biopores or the soil matrix without biopores in the immediate neighbourhood (Figure 2). In the chicory treatment, the drilosphere and the bulk soil showed similar low pO_2 values while the rhizosphere had around 7 kPa higher pO_2 levels. In the alfalfa treatment, the drilosphere had the lowest pO_2 levels, around 5 kPa lower than the bulk soil and 10 kPa lower than the

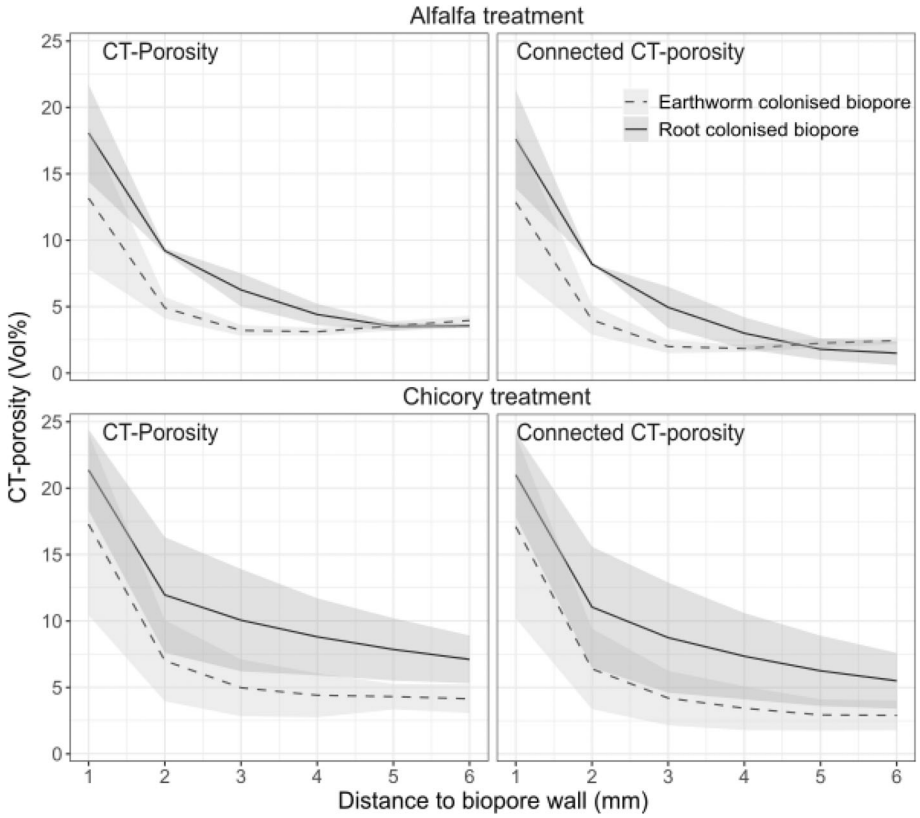

FIGURE 4 CT-porosity and biopore-connected CT-porosity as function of the distance to the biopore's surface as calculated from the X-ray CT images of the very same samples as in Figures 2 and 3. Lines are average values and shaded regions represent the standard error of mean ($n = 3$).

rhizosphere. Figure 3 shows D_S/D_O measured at one to six millimetres distance from the biopore wall into the soil matrix. For the chicory treatment, D_S/D_O is greater near a root colonised biopore than near an earthworm colonised biopore or in the bulk soil. With increasing distance from the biopore wall, D_S/D_O remained higher for the root colonised biopore compared to the other microsites up to a depth of 5 mm. This was due to the higher number of lateral channels around root colonised biopores which was confirmed by the X-ray CT image analysis (Figure 4). Similar results were determined for the alfalfa treatment, however, with an increased effect on D_S/D_O (notice the different Y-axis scales in Figure 3), up to a depth of 4 mm from the biopore wall.

The difference in lateral CT-porosity between both types of biopores could also be observed and quantified in the X-ray CT images. Figure 4 shows differences in lateral CT-porosity between biopores colonised by earthworms and by roots. Lateral CT-porosity of the root colonised biopore was higher than for the earthworm colonised biopore. This could be observed in both treatments. Also, the difference between the total lateral CT-porosity and the connected lateral CT-porosity is less for the root colonised biopore than for the earthworm biopore. This means that most of the pore space around the root colonised biopores is connected to the main biopore which in turn is connected to the free atmosphere. The higher number of lateral channels around the root colonised biopore improves aeration from the biopore surface to the soil matrix as was observed in the D_S/D_O measurements.

4 | DISCUSSION

Although it is widely known that soil physical properties are considerably influenced by roots and macrofauna (Angers & Caron, 1998), there are still gaps in the qualitative description and quantification of microstructural characteristics of the rhizodrilosphere such as pore size distribution, pore geometries and connectivity and their implication for gas transport. Both macrofauna and roots are assumed to compact the soil around biopores which would have a negative impact on the gas exchange and accessibility of surfaces inside the "bulk soil" amongst others. But in the case of roots, their secondary lateral pores create connected channels and reorient particles because of intensified shrink and swell cycles (as described in Horn & Dexter, 1989) which promote aggregation and hence modify pore size distributions. On the other side, earthworms generate completely different biopores. By mixing soil and organic matter and excreting them, they smear the compacted surfaces of the biopore, thus no new lateral channels are created and existing

ones are clogged. As microscale structures are intimately linked to soil functional processes, characteristics have to be analysed in connection with pore functionality which was not done until now.

In this study, we observed that roots altered their surrounding soil pore geometries to a greater extent than earthworms would do. This is in accordance with (Hinsinger et al., 2009) who suggested that roots create microsites especially adapted for life. In addition, Lucas et al. (2019b) could show that changes in soil physical properties in the rhizosphere generate feedback mechanisms on root development (e.g., changes in mechanical and hydraulic properties that both influence root growth). This includes microbiological and geochemical processes that in turn will have an influence on nutrient supply and plant performance. In our study, we complement this information by showing how roots create structural porosity and biopores that are added to the existing matrix porosity affecting to a great extent oxygen-related processes in the rhizosphere. The processes of macropore generation are clearly time-dependent and follow direct and indirect biotic mechanisms. Structural pores related to cracks occur when the tensile stress exceeds the internal soil strength through hydraulic stress, which in the subsoil is triggered by root water extraction (Horn, 2004). Root water uptake intensified by dry periods may induce proportional shrinkage beyond the limit of the structural shrinkage range. As a direct mechanism, we observe lateral roots creating holes as they grow. Both mechanisms are intensified over time as new pore structures are generated (Lucas et al., 2019a). Macroporosity at the pedon scale can be significantly increased already after two to three cultivation years of the used treatments in this study (Uteau et al., 2013). Thus, it is possible that differentiation of porosity in the millimetre scale occurs right after one growing period. According to the findings of this study, two years were enough to show a differentiation between earthworm and root colonised biopores. Our results were not tested for significant differences because of the lack of replicates. Nevertheless, it is to the best of our knowledge, the first time that a direct link between soil microstructural (X-ray CT and image analysis) and functional properties (microscale oxygen distribution and diffusion) of a naturally formed rhizophere and drilosphere was demonstrated. Our study clearly shows the differentiation of the pore geometries between both types of biopores resulting in a strong modification of oxygen fluxes between biopore surfaces and their surrounding soil.

The present findings have significant implications for oxygen supply in deeper layers of the soil. Roots consume oxygen for many processes, but the most important one is root growth, as confirmed by many authors (e.g., Anderson & Kemper, 1964; Bertrand & Kohnke, 1957; Dinneny, 2019; Gradwell, 1965). The consumption may vary according to the energy necessary for the physiological process. Some relevant factors affecting root respiration are oxygen concentration, fertilisation and mechanical impedance (Glinski & Stepniewski, 1985). Dorau et al. (2022) found a threshold of 2% connective air-filled CT-porosity to be enough to switch from reducing to oxidising conditions. This threshold is given here for both studied microsites (Figure 4), but it does not account for the absolute amount of consumed oxygen. As could be observed in laboratory experiments, rhizosphere respiration (microbial and root respiration) can decrease by a factor of 100 if the oxygen concentration is lower than 3% (Uteau et al., 2015). Although it was not possible to separate microbial from root respiration, it can be interpreted from such experiments, that root growth and microbial activities are inhibited under hypoxic conditions. Further studies found the highest microbiological activity in well-aerated and nutrient-rich zones as biopores (Kuzyakov, 2010; Nunan et al., 2003) making it extremely important with respect to the oxygen supply. But such studies do not distinguish between root and earthworm colonised biopores. Here it is shown that, with respect to aeration, this differentiation matters (Figures 2–4). This finding is highly relevant as microbial activity plays a fundamental role in the mineralization of organic matter, degradation of contaminants and regulation of N and C cycles (Brzezińska et al., 1998; Jones et al., 2004; Pausch & Kuzyakov, 2011). At low oxygen levels, microbes switch from aerobic to facultative anaerobic respiration and all mineralization processes are slowed down, directly affecting fertility. Also low redox potential inhibits root nutrient uptake (Drew et al., 1988; Fiedler et al., 2007) which should not occur if the pores surrounding the roots are connected to the main biopore which in turn is connected to the free atmosphere (Dorau et al., 2022) as shown in our study (Figure 4).

Our study presents several limitations due to the natural condition of the soil (undisturbed soil cores of a naturally structured soil) and variables that we were not able to control, such as worm species and the real age of the biopores and lateral channels. Nevertheless, we considered it relevant to shift from classical homogenised repacked columns (e.g., Rogasik et al., 2014) and explore more near-to-field conditions showing real pore networks existing in arable soils as suggested in several studies (e.g., Andriuzzi et al., 2013; Pagenkemper et al., 2015). Despite these limitations, we could measure differences in the lateral CT-porosity of biopores depending on their type which should be investigated deeply in further studies.

5 | CONCLUSIONS

The combination of microstructural analysis of 3D pore spaces in the rhizosphere and drilosphere with microsensor measurements of oxygen partial pressures and D_S/D_O were suitable to assess differences in the aeration conditions in different microsites of naturally structured soil. Aeration was considerably enhanced in the soil matrix surrounding biopores in comparison to the bulk soil, shown by higher oxygen concentrations and higher D_S/D_O. While biopores colonised by earthworms are characterised by well compacted, sheared, and organic casts, polished pore walls with minor links to the adjacent soil volume, biopores colonised by roots presented more connected lateral pores that enhanced D_S/D_O into the soil matrix resulting in a better supply of oxygen. This has implications for biotic processes that depend on gas exchange as microbial turnover and mineralization or also root respiration at the root-soil interface. Similar results were obtained independently of the studied crops (alfalfa and chicory). Further studies should have better control on the genesis of the biopores and an increased number of replicates to allow for statistical analysis.

AUTHOR CONTRIBUTIONS

Daniel Uteau: Conceptualization (equal); data curation (lead); formal analysis (lead); investigation (equal); methodology (lead); validation (lead); writing – original draft (lead); writing – review and editing (lead). **Rainer Horn:** Conceptualization (equal); funding acquisition (lead); investigation (supporting); methodology (supporting); project administration (lead); resources (lead); supervision (lead); writing – original draft (supporting); writing – review and editing (supporting). **Stephan Peth:** Conceptualization (equal); funding acquisition (lead); investigation (equal); methodology (supporting); project administration (lead); resources (supporting); supervision (lead); writing – original draft (supporting); writing – review and editing (supporting).

ACKNOWLEDGEMENTS

We thank Dr. Lars Larsen (Unisense A/S, Denmark) for his support in the setup of the oxygen microsensors. This study was possible thanks to the sponsoring of the German Research Foundation (Deutsche Forschungsgemeinschaft, DFG) within the framework of the Package Proposal "Small scaled and dynamic analyses of microstructural rhizo- and drilosphere properties: porosity, physicochemistry and their role for root growth, nutrient storage and transport/support" (DFG PAK888). Open Access funding enabled and organized by Projekt DEAL.

CONFLICTS OF INTEREST

The authors declare that there is no conflict of interest that could be perceived as prejudicing the impartiality of the research reported.

DATA AVAILABILITY STATEMENT

The data used in this study is available upon request from the corresponding author. The data set will be archived for at least 10 years after publication.

ORCID

Daniel Uteau https://orcid.org/0000-0003-1499-4344

REFERENCES

Anderson, W. B., & Kemper, W. D. (1964). Corn growth as affected by aggregate stability, soil temperature, and soil moisture. *Agronomy Journal*, *56*, 453–456.

Andriuzzi, W. S., Bolger, T., & Schmidt, O. (2013). The drilosphere concept: Fine-scale incorporation of surface residue-derived N and C around natural *Lumbricus terrestris* burrows. *Soil Biology and Biochemistry*, *64*, 136–138.

Angers, D. A., & Caron, J. (1998). Plant-induced changes in soil structure: Processes and feedbacks. *Biogeochemistry*, *42*, 55–72.

Beck-Broichsitter, S., Fleige, H., Dusek, J., & Gerke, H. H. (2020). Anisotropy of unsaturated hydraulic properties of compacted mineral capping systems seven years after construction. *Soil and Tillage Research*, *204*, 104702.

Bertrand, A. R., & Kohnke, H. (1957). Subsoil conditions and their effects on oxygen supply and the growth of corn roots. *Soil Science Society of America Journal*, *21*, 135–140.

Bruand, A., Cousin, I., Nicoullaud, B., Duval, O., & Begon, J. C. (1996). Backscattered electron scanning images of soil porosity for analyzing soil compaction around roots. *Soil Science Society of America Journal*, *60*, 895–901.

Brzezińska, M., Stępniewska, Z., & Stępniewski, W. (1998). Soil oxygen status and dehydrogenase activity. *Soil Biology and Biochemistry*, *30*, 1783–1790.

Butt, K. R., & Grigoropoulou, N. (2010). Basic research tools for earthworm ecology. *Applied and Environmental Soil Science*, *2010*, e562816. https://doi.org/10.1155/2010/562816

Carminati, A., Schneider, C. L., Moradi, A. B., Zarebanadkouki, M., Vetterlein, D., Vogel, H.-J., Hildebrandt, A., Weller, U., Schüler, L., & Oswald, S. E. (2011). How the rhizosphere may favor water availability to roots. *Vadose Zone Journal*, *10*, 988–998.

Carminati, A., Vetterlein, D., Weller, U., Vogel, H.-J., & Oswald, S. E. (2009). When roots lose contact. *Vadose Zone Journal*, *8*, 805–809.

Dinneny, J. R. (2019). Developmental responses to water and salinity in root systems. *Annual Review of Cell and Developmental Biology*, *35*, 239–257. https://doi.org/10.1146/annurev-cellbio-100617-062949

Dorau, K., Uteau, D., Hövels, M., Peth, S., & Mansfeldt, T. (2022). Soil aeration and redox potential as function of pore connectivity unravelled by X-ray microtomography imaging. *European Journal of Soil Science*, *73*(1), e13165. https://doi.org/10.1111/ejss.13165

Dorioz, J. M., Robert, M., & Chenu, C. (1993). The role of roots, fungi and bacteria on clay particle organization. An experimental approach. *Geoderma*, *56*, 179–194.

Dörner, J., & Horn, R. (2009). Direction-dependent behaviour of hydraulic and mechanical properties in structured soils under conventional and conservation tillage. *Soil and Tillage Research*, *102*, 225–232.

Drew, M. C., Guenther, J., & Läuchli, A. (1988). The combined effects of salinity and root anoxia on growth and net Na+ and K+-accumulation in Zea mays grown in solution culture. *Annals of Botany*, *61*, 41–53.

Eden, M., Moldrup, P., Schjønning, P., Scow, K. M., & de Jonge, L. W. (2012). Soil-gas phase transport and structure parameters for a soil under different management regimes and at two moisture levels. *Soil Science*, *177*, 527–534.

Fiedler, S., Vepraskas, M. J., & Richardson, J. L. (2007). Soil redox potential: Importance, field measurements and, observations. In *Advances in agronomy* (pp. 1–54). Academic Press.

Glinski, J., & Stepniewski, W. (1985). *Soil aeration and its role for plants*. CRC Press.

Gradwell, M. W. (1965). Soil physical conditions of winter and the growth of ryegrass plants: I. effects of compaction and puddling. *New Zealand Journal of Agricultural Research*, *8*, 238–269.

Haas, C., & Horn, R. (2018). Impact of small-scaled differences in micro-aggregation on physico-chemical parameters of macroscopic biopore walls. *Frontiers in Environmental Science*, *6*, 90.

Hackett, C. (1982). *Edible horticultural crops: A compendium of information on fruit, vegetable, spice, and nut species*. Academic Press, Sydney.

Han, E., Kautz, T., Perkons, U., Uteau, D., Peth, S., Huang, N., Horn, R., & Köpke, U. (2015). Root growth dynamics inside and outside of soil biopores as affected by crop sequence determined with the profile wall method. *Biology and Fertility of Soils*, *51*, 847–856.

Heichel, G. H. (1980). Alfalfa. In D. Pimentel (Ed.), *Handbook of energy utilization in agriculture* (pp. 155–161). CRC Press c1980.

Helliwell, J. R., Sturrock, C. J., Miller, A. J., Whalley, W. R., & Mooney, S. J. (2019). The role of plant species and soil condition in the structural development of the rhizosphere. *Plant, Cell & Environment*, *42*(6), 1974–1986. https://doi.org/10.1111/pce.13529

Hinsinger, P., Bengough, A., Vetterlein, D., & Young, I. (2009). Rhizosphere: Biophysics, biogeochemistry and ecological relevance. *Plant and Soil*, *321*, 117–152.

Horn, R. (1994, 1994). Effect of aggregation of soils on water, gas and heat transport. In E. D. Schulze (Ed.), *Flux control in biological systems: From enzymes to populations and ecosystems* (pp. 335–361). Academic Press.

Horn, R. (2004). Time dependence of soil mechanical properties and pore functions for arable soils. *Soil Science Society of America Journal*, *68*, 1131–1137.

Horn, R., & Dexter, A. R. (1989). Dynamics of soil aggregation in an irrigated desert loess. *Soil and Tillage Research*, *13*, 253–266.

Horn, R., & Peth, S. (2009). Soil structure formation and management effects on gas emission. *Biologia*, *64*, 449–453.

Horn, R., Taubner, H., Wuttke, M., & Baumgartl, T. (1994). Soil physical properties related to soil structure. *Soil and Tillage Research*, *30*, 187–216.

IUSS (Internation Union of Soil Science) Working Group WRB. (2015). World reference base for soil resources 2014, update 2015. International soil classification system for naming soils and creating legends for soil maps. World Soil Resources report 106. FAO. Rome.

Jones, D. L., Hodge, A., & Kuzyakov, Y. (2004). Plant and mycorrhizal regulation of rhizodeposition. *New Phytologist*, *163*, 459–480.

Kirkegaard, J., Christen, O., Krupinsky, J., & Layzell, D. (2008). Break crop benefits in temperate wheat production. *Field Crops Research*, *107*, 185–195.

Kutschera, L. & Lichtenegger, E. (1992). Wurzelatlas mitteleuropäischer Grünlandpflanzen. Band 2. Pteridophyta und Dicotyledoneae. G. Fischer, Stuttgart.

Kuzyakov, Y. (2010). Priming effects: Interactions between living and dead organic matter. *Soil Biology and Biochemistry*, *42*, 1363–1371.

Larney, F. (2007). Dry-aggregate size distribution. In M. Carter & E. Gregorich (Eds.), *Soil sampling and methods of analysis* (Second ed., pp. 821–832). CRC Press.

Lucas, M., Schlüter, S., Vogel, H.-J., & Vetterlein, D. (2019a). Soil structure formation along an agricultural chronosequence. *Geoderma*, *350*, 61–72.

Lucas, M., Schlüter, S., Vogel, H.-J., & Vetterlein, D. (2019b). Roots compact the surrounding soil depending on the structures they encounter. *Scientific Reports*, *9*, 16236.

Materechera, S. A., Alston, A. M., Kirby, J. M., & Dexter, A. R. (1992). Influence of root diameter on the penetration of seminal roots into a compacted subsoil. *Plant and Soil*, *144*, 297–303.

Nunan, N., Wu, K., Young, I. M., Crawford, J. W., & Ritz, K. (2003). Spatial distribution of bacterial communities and their relationships with the micro-architecture of soil. *FEMS Microbiology Ecology*, *44*, 203–215.

Oades, J. M. (1993). The role of biology in the formation, stabilization and degradation of soil structure. *Geoderma*, *56*, 377–400.

Otsu, N. (1979). A threshold selection method from gray-level histograms. *IEEE Transactions on Systems, Man, and Cybernetics*, *9*, 62–66.

Pagenkemper, S. K., Athmann, M., Uteau, D., Kautz, T., Peth, S., & Horn, R. (2015). The effect of earthworm activity on soil bioporosity – Investigated with X-ray computed tomography and endoscopy. *Soil and Tillage Research*, *146*, 79–88.

Pausch, J., & Kuzyakov, Y. (2011). Photoassimilate allocation and dynamics of hotspots in roots visualized by ^{14}C phosphor imaging. *Journal of Plant Nutrition and Soil Science*, *174*, 12–19.

Peth, S., Horn, R., Beckmann, F., Donath, T., Fischer, J., & Smucker, A. J. M. (2008). Three-dimensional quantification of intra-aggregate pore-space features using synchrotron-radiation-based microtomography. *Soil Science Society of America Journal*, *72*, 897–907.

Pietola, L. M., & Smucker, A. J. M. (1995). Fine root dynamics of alfalfa after multiple cuttings and during a late invasion by weeds. *Agronomy Journal*, *87*, 1161–1169.

Rappoldt, C. (1995). Measuring the millimetre-scale oxygen diffusivity in soil using microelectrodes. *European Journal of Soil Science*, *46*, 169–177.

Rasse, D. P., & Smucker, A. J. M. (1998). Root recolonization of previous root channels in corn and alfalfa rotations. *Plant and Soil*, *204*, 203–212.

Rasse, D. P., Smucker, A. J. M., & Santos, D. (2000). Alfalfa root and shoot mulching effects on soil hydraulic properties and aggregation. *Soil Science Society of America Journal*, *64*, 725–731.

Rogasik, H., Schrader, S., Onasch, I., Kiesel, J., & Gerke, H. (2014). Micro-scale dry bulk density variation around earthworm (*Lumbricus terrestris* L.) burrows based on X-ray computed tomography. *Geoderma*, *213*, 471–477.

Uteau, D., Hafner, S., Pagenkemper, S. K., Peth, S., Wiesenberg, G. L. B., Kuzyakov, Y., & Horn, R. (2015). Oxygen and redox potential gradients in the rhizosphere of alfalfa grown on a loamy soil. *Journal of Plant Nutrition and Soil Science*, *178*, 278–287.

Uteau, D., Pagenkemper, S. K., Peth, S., & Horn, R. (2013). Root and time dependent soil structure formation and its influence on gas transport in the subsoil. *Soil and Tillage Research*, *132*, 69–76.

White, R. G., & Kirkegaard, J. A. (2010). The distribution and abundance of wheat roots in a dense, structured subsoil and implications for water uptake. *Plant, Cell & Environment*, *33*, 133–148.

Young, I. M. (1998). Biophysical interactions at the root–soil interface: A review. *The Journal of Agricultural Science*, *130*, 1–7.

Yunusa, I. A. M., & Newton, P. J. (2003). Plants for amelioration of subsoil constraints and hydrological control: The primer-plant concept. *Plant and Soil*, *257*(2), 261–281.

SUPPORTING INFORMATION

Additional supporting information can be found online in the Supporting Information section at the end of this article.

How to cite this article: Uteau, D., Horn, R., & Peth, S. (2022). Millimetre scale aeration of the rhizosphere and drilosphere. *European Journal of Soil Science*, *73*(4), e13269. https://doi.org/10.1111/ejss.13269